Published in final edited form as:
Somatosens Mot Res. 2008 September ; 25(3): 149–162. doi:10.1080/08990220802249275.

Multiple Parietal Operculum Subdivisions in Humans:

Tactile Activation Maps

Harold Burton[1,2], **Robert J. Sinclair**[1], **Jason R. Wingert**[1], and **Donna L. Dierker**[1]

1*Department of Anatomy and Neurobiology, Washington University School of Medicine, St. Louis, MO 63110*

2*Department of Radiology, Washington University School of Medicine, St. Louis, MO 63110*

Abstract

We focused the present analysis on blood oxygen-level dependent responses evoked in four architectonic subdivisions of human posterior parietal operculum (PO) during two groups of tasks involving either vibrotactile stimulation or rubbing different surfaces against the right index finger pad. Activity localized in previously defined parietal opercular subdivisions, OP 1-4 was co-registered to a standard cortical surface-based atlas. Four vibrotactile stimulation tasks involved attention to the parameters of paired vibrations: (1) detect rare target trials when vibration frequencies matched; (2) select the presentation order of the vibration with a higher frequency or (3) longer duration; and (4) divide attention between frequency and duration before selecting stimulus order. Surface stimulation tasks involved various discriminations of different surfaces: (1) Smooth surfaces required no discrimination. (2) Paired horizontal gratings required determination of the direction of roughness change. (3) Paired shapes entailed identifying matched and unmatched shapes. (4) Raised letters involved letter recognition. The results showed activity in multiple somatosensory subdivisions bilaterally in human PO that are plausibly homologues of somatosensory areas previously described in animals. All tasks activated OP 1, but in vibrotactile tasks foci were more restricted compared to moving surface tasks. Greater spatial extents of activity especially in OP 1 and 4 when surfaces rubbed the finger pad did not support previously reported somatotopy of the second finger representation in "S2." The varied activity distributions across OP subdivisions may reflect low level perceptual and/or cognitive processing differences between tasks.

Keywords

human parietal cortex; magnetic resonance imaging; touch

INTRODUCTION

Brain imaging studies have confirmed somatosensory evoked responses in human parietal operculum that are in addition to those recorded along the postcentral gyrus. In concordance with studies in nonhuman primates, the parietal opercular activity was identified as human "S2" (Burton et al., 1993; Ledberg et al., 1995). But the human parietal opercular cortical subdivision consists of multiple cytoarchitectonic areas (Disbrow et al., 2000; Disbrow et al., 2003; Eickhoff et al., 2006a; Eickhoff et al., 2006b) that have been considered homologues to subdivisions identified in monkeys: OP 1 to S2, OP 2 to an inferior parietal vestibular area

Send all communications to: Dr. H. Burton, Department of Anatomy and Neurobiology, Campus Box 8108, Washington University School of Medicine660 South Euclid Avenue, St. Louis, MO 63110, Phone: (314) 362-3556, Fax: (314) 747-4370, E-Mail: harold@pcg.wustl.edu.

(PIVC), OP 3 to a ventral somatosensory area, VS, and OP 4 to a parietal ventral area, PV (Eickhoff et al., 2006a; Eickhoff et al., 2006c; Eickhoff et al., 2007).

Similar somatotopic organizations have been noted in S2 and PV subdivisions of monkeys (Burton et al., 1995; Coq et al., 2004; Disbrow et al., 2003; Krubitzer et al., 1995; Qi et al., 2002; Robinson and Burton, 1980a; Wu and Kaas, 2003) and OP 1 and OP 4, respectively, of humans (Disbrow et al., 2000; Eickhoff et al., 2007). Generally, a mirror reversed somatotopy between S2 and PV in monkeys also has been noted between OP 1 and OP 4 in humans (Eickhoff et al., 2007). The reversal occurs at subdivision borders and reflects representations for distal body anatomy and head with surrounding representations for more proximal body parts (Eickhoff et al., 2007). In this pattern digits are represented through the middle of the parietal operculum, across the border between OP 1 and OP 4 (Eickhoff et al., 2007; Ruben et al., 2001; Young et al., 2004), and comparably across the border between S2 and PV in monkeys (Burton et al., 1995; Coq et al., 2004; Disbrow et al., 2003; Krubitzer et al., 1995; Qi et al., 2002; Robinson and Burton, 1980a; Wu and Kaas, 2003) and other species (Krubitzer et al., 1986; Krubitzer and Calford, 1992).

OP 3 is located at the fundus of the parietal operculum and responds to tactile stimulation (Eickhoff et al., 2006a; Eickhoff et al., 2006b; Eickhoff et al., 2007). VS, the putative monkey homologue of OP 3, has rostral and caudal components that respectively are located medial to PV and S2 (Coq et al., 2004; Wu and Kaas, 2003). VS-caudal has an anterior to posterior/trigeminal to lumbar-sacral somatotopy along the fundus of the lateral sulcus (Coq et al., 2004; Qi et al., 2002; Wu and Kaas, 2003) that resembles the topography previously reported for the retroinsular cortex (Ri) in macaques (Robinson and Burton, 1980b). However, only a hint of a rostro-caudal somatotopy has been noted in OP 3 (Eickhoff et al., 2007). Unlike VS-caudal, OP 3 lies medial to OP 4/PV. A vestibular representation in OP 2 occupies the fundal region medial to OP 1/S2 (Eickhoff et al., 2006c).

Human “S2” responds to manually applied tactile stimulation even without task relevance (Disbrow et al., 2000; Eickhoff et al., 2006d; Eickhoff et al., 2007; Ruben et al., 2001). Cognitively relevant tasks elicit greater activation (Bodegård et al., 2000; Bodegård et al., 2001; Burton et al., 2008; Ledberg et al., 1995; Nelson et al., 2004; Reed et al., 2005; Roland et al., 1998; Young et al., 2004). Sensory linked motor behaviors also evoke responses in “S2” (Binkofski et al., 1999; Hinkley et al., 2007; Inoue et al., 2002; Wasaka et al., 2005).

A central question regarding lateral parietal somatosensory areas is whether they selectively and distinguishably respond to different tactile stimulation paradigms. The current analysis was especially aided because all individual fMRI data were coincidently registered to OP cytoarchitectonic subdivisions using a surface-based atlas of the human cerebral cortex (Van Essen, 2005). Additionally, activity was examined using servo-controlled stimulation of the same right index finger pad in two different protocols. We contrasted results between one set of tasks that utilized vibrotactile, punctate stimulation and a second set that involved moving surface stimulation. Cognitive complexity also varied across the tasks, which allowed contrasts between tasks with fewer and greater discrimination demands. We selectively focused on newly defined human opercular regions with the goal of determining whether each is differentially affected by varied cognitive and stimulation factors.

MATERIALS and METHODS

The present analysis focused on activity evoked in the parietal operculum by tactile stimulation of an extended, passively restrained right index finger. All image acquisition synchronized to tasks presented with single event designs (Table 1).

For Tasks 1, 2-4, 5-7, and 8 we recorded activity in, respectively 8, 12, 10 and 10 different adults (Table 1) who gave consent in accordance with Washington University Human Studies Committee guidelines. Participants self-reported no history of neurological conditions or head trauma, no current medications, and no contraindication to MRI. All but one participant was right-handed based on responses to a modified Edinburgh handedness inventory (Raczkowski et al., 1974) (Table 1, a score of 100 indicates complete right-handedness).

In the tasks utilizing vibrotactile stimulation, a servo-controlled vibrator (Figure 1A1) applied sinusoidal vibrations through a 3.5 mm diameter flat plastic probe tip (Burton et al., 2004, 2008). The tip contacted the skin through a platform (Figure 1A2) with a 5.5 mm hole, leaving a 1 mm annulus. Vibration amplitudes were suprathreshold and individually adjusted for subjective intensity equalization across applied frequencies.

A similar temporal structure governed all vibrotactile stimulation tasks in which individual trials involved presentation of paired vibrations (Figure 2A, B). Behavioral responses, whether overt with the left hand or covert, were required after each trial. Three closely spaced successive trials were followed by a longer interval with no stimulation. Collectively the three trials and following no-stimulation interval were analyzed as a single long duration event.

For Task 1 (Figure 2A) participants detected whether the paired vibrations in a trial had identical frequencies. Such trials were rare (~7% incidence or 17/240 trials across four imaging runs). Detections were signaled by elevating the left second finger; trials with unmatched frequencies were signaled by refraining from any left finger movement. The test frequencies were 25 or 100 Hz with displacement amplitudes of 130 and 35μm, respectively. The number of 25 and 100Hz presentations was equal across and within imaging runs.

In Task 1 each vibration lasted 750ms, 300ms gaps separated vibrations in a trial, and 1.5sec intervals separated neighboring trials. Three sequential vibration trials were followed by a ~14sec interval of no stimulation. Collectively these were analyzed as single ~23s events (Figure 2A). A “target event” contained at least one trial where vibration frequencies matched. A “non-target event” involved three sequential trials of un-matched paired frequencies. For the present analysis we examined activity evoked during the more prevalent “non-target events.”

For Tasks 2-4 participants decided whether a larger value of a cued parameter occurred first or second within a trial (Burton et al., 2008). Selective cuing directed participant attention to the parameters of vibration frequency and duration in Tasks 2 and 3, respectively. The target vibration was stimulation with a higher frequency for Task 2 and stimulation presented with a longer duration for Task 3. A non-informative cue (e.g., neutral cuing) in Task 4 required that participants divide attention between both vibration parameters to identify the stimulus order of the one that changed. On trials with a selective cue, vibration frequency and duration values were manipulated on every trial, but only the values of the cued attribute were relevant. Three sequential trials were similarly cued, but the temporal order of the targeted parameter values was randomly determined for every trial.

In Tasks 2-4 the duration of each vibration varied (see below), 500ms gaps separated vibrations in a trial, and 3sec intervals separated neighboring trials. Three sequential and similarly cued trials and a following 13sec no-stimulation interval were collectively analyzed as a single ~28s event (Figure 2B). Event types were defined by cue type, which was randomized within runs. There were 32 events per type that were equally distributed across four imaging runs.

Attention to the frequency parameter involved two standards. The low frequency standard was 25Hz (SEM: ±0Hz; amplitude mean and SEM: 130μm ±27.5), which was paired with a vibration whose mean was either 14Hz (±1.1Hz; 134μm ±21.3) or 36Hz (±1.3Hz; 106μm

±20.8); and a high frequency standard of 180Hz (±11.3Hz; 30μm ±2.6) was paired with a vibration whose mean was 136Hz (±12.6Hz; 38μm ±5.2) or 238Hz (±14.2Hz; 29μm ±3.5). Attention to vibration duration involved a single 1000ms standard. The comparison mean shorter interval was 960.4ms (±4.2) and the mean longer interval was 1041ms (±4.2). The range of vibration amplitudes, frequencies and durations noted above reflected adjustments needed to obtain 75% accuracy in every participant for every task during over-training in prior non-imaging sessions.

Participants overtly pushed different buttons to signal the target order in training sessions when performance data were obtained. During imaging participants covertly thought 1 or 2 when detecting a target order of first or second of paired stimulation. All participants reported after the scans that the tasks and their perceived target detections were comparable to what they experienced during training sessions.

Trials were visually cued, and cues were continuously present during stimulation in each event (Figure 2B). During imaging the cues were words printed in white below a white cross and against a unique colored background. When selectively cuing frequency (Task 2) the screen showed “FREQ” against a green background; during selective cuing for duration (Task 3) the screen word was “TIME” against a red background; and for neutral cuing (Task 4) the word was “BOTH” against a screen divided into top half green and bottom half red. The screen was black otherwise except for a white cross.

In the tasks (5-8) utilizing surface stimulation, a servo-controlled rotating drum (Burton et al., 2006) translated a photopolymer printing material across the finger pad from proximal to distal (Figure 1B1). The finger rested in a channel that aligned the finger pad with a track along the drum belt containing a selected pattern (Figure 1B2). Tracks consisted of continuous smooth or interrupted embossed patterns (elevated ~0.8mm) arranged in short lengths separated by smooth segments on a 330cm flexible belt. Drum speeds were 22 and 30mm/s, respectively for Tasks 5-7 and 8.

The temporal structure of all surface stimulation tasks was similar (Figure 2C, D). Each trial encompassed a fixed interval of surface movement that included initial rotary acceleration, constant velocity, deceleration, and a variable interval with no movement when the finger contacted a smooth surface. Overt behavioral responses occurred after movement stopped. Collectively the interval of surface movement, behavioral response and a variable duration of post-movement rest were analyzed as single events. Timing between events was jittered by changing the duration of post-movement intervals. The distribution of these intervals followed a truncated negative exponential distribution. Total event durations ranged from 12.3-22.5s for Tasks 5-7 and 15-27.5s for Task 8. Each event was synchronized with image acquisitions. Analyses (Miezin et al., 2000; Ollinger et al., 2001a; Ollinger et al., 2001b) considered average event durations of 17.5 and 20sec, respectively for Tasks 5-7 and Task 8 (Figure 1C, D).

In Task 5 a continuous smooth surface rubbed across the finger; no surface pattern discriminations were required for this task. Participants pushed a response key on every trial upon hearing a chime with either the left second or third fingers on alternative runs.

In Task 6 embossed 40mm strips of horizontal gratings with variable groove widths and constant ridge widths of ~250μm rubbed against the skin. These strips consisted of two equal lengths that differed in groove widths (gratings with wider groove widths feel rougher). The task required detecting the direction of roughness change. In all trials a 1000μm groove width standard was compared to gratings with groove widths of 1800-2900μm (i.e., six groove width differences between 800-1900μm). Each direction of change and each combination of groove width differences was equally probable (i.e., standard touched first or second). Events

encompassed stimulation with one 40mm grating strip and participant button push responses to signal perceived direction of roughness change (Figure 2C).

In Task 7 four sequential embossed shapes along a 40mm length were rubbed against the skin. The same shapes were touched in pairs, and two sequential pairs were presented during each trial. The task involved recognizing whether touched shapes matched. Three 8 × 8 mm shapes were used (circle, three-sided open square, and a V). Example combinations were circle-circle vs. circle-circle, open square - open square vs. circle-circle, etc. Whether shapes in the second pair matched those in the first varied randomly with equal probability. An event included moving the shapes across the finger and participant button push response to indicate yes or no regarding whether the shapes matched (Figure 2C).

Left and right button pushes signaled direction of roughness change for Task 6 and match-no-match for Task 7. Buttons had reverse designations for half of the participants. The linkage between specified button pushes and the two alternative choices was counterbalanced across the participants. For Tasks 5-7 a chime heard during drum deceleration signaled when to push a button (Figure 2C).

In Task 8 a string of 6 identical embossed capital letters rubbed across the skin (Burton et al., 2006). Target letters were A, I, J, L, O, T, U and W, which are the least confusable when passively translated across a finger (Vega-Bermudez et al., 1991). Letters in block capital Arial font were 8 mm high and letter dependent variable widths. Events consisted of translating the string with letters presented in a top-to-bottom direction followed by a pause in rotation during which participants vocally identified the letter (Figure 2D).

Image processing

We imaged blood oxygenation level-dependent (BOLD) contrast responses (Kwong et al., 1992; Ogawa et al., 1990) using asymmetric spin-echo, echo-planar sequences (EPI) in a 1.5T Vision scanner for Tasks 2-4 and a 3T Allegra scanner (Siemens, Erlangen, Germany) for all other tasks (Table 1). Whole brain coverage was obtained using contiguous, interleaved axial slices, oriented parallel to the bicommissural plane. Sagittal, T1-weighted magnetization prepared rapid gradient echo (MP-RAGE) images (1 × 1 × 1.25mm) were used for atlas transformation and cortical segmentation in each participant.

Preprocessing all fMRI data corrected for head motion within and across runs, adjusted intensity differences due to interleaved slice acquisition, normalized global mean signal intensity across runs, and compensated for slice-dependent time shifts using sync interpolation.

Registration of each structural MRI volume to the 711-2B atlas (Buckner et al., 2004) was through computed affine transforms that linked the first image volume of each EPI run (averaged over all runs after cross-run realignment) with the MP-RAGE images (Ojemann et al., 1997). Images were re-sampled in atlas space to 2 mm^3 isotropic voxels and spatially smoothed (4 mm FWHM) before statistical analyses.

Statistical Analyses

Estimates of the per cent MR signal change per voxel for the time points of an event relative to baseline activity was obtained for each event-type using a general linear model (GLM). Separate GLMs were computed for Tasks 1, 2-4, 5-7 and 8 because each group of tasks involved different event durations (Figure 2A-D). Each GLM contained regressors for the time points in specified events, linear drift in MR signal across concatenated runs, and a high-pass filter.

Because the temporal structure of events differed (Figure 2A-D), we did not contrast results between tasks based on standard response magnitudes, which usually are obtained from

convolving evoked BOLD responses with a canonical hemodynamic response function (Friston et al., 1995). Instead we assessed activity using an F-test, which evaluated whether variance in percent change of MR signal relative to baseline during a particular event-type accounted for a greater proportion of summed variance than variance from a corresponding interval of baseline activity (noise). Larger F-ratio magnitudes indicate BOLD responses evoked during events accounted for a greater proportion of recorded MR variance. F-ratios were transformed to normalized z-scores (e.g., F-test z-scores).

F-test z-scores were evaluated in two ways. First, group whole-brain activation analysis was obtained for each task using a random effect T-map of the F-test z-scores (Holmes and Friston, 1998). Second, the spatial extent of activity thresholded for significance in each OP region by task was assessed. An index computed from these spatial extent measurements (see below) provided a dependent variable for task contrasts in random effect ANOVA and post-hoc t-tests. Both random effects analyses were performed after registering the voxelwise F-test z-scores to the cortical surface of each individual.

Surface mapping

We generated a fiducial cortical surface per hemisphere for each individual using the SureFit algorithm in Caret (Van Essen et al., 2001). The voxelwise F-test z-scores were then registered to surface nodes based on coordinate intersection of surface nodes enclosed by that voxel (Burton et al., 2008). Next, F-test z-scores at each participant-specific cortical surface node were re-sampled to the PALS-B12 standard mesh using nearest node metric mapping. The latter was accomplished after participant-specific surfaces were registered to the PALS-B12 atlas using six standard landmarks and a spherical registration algorithm applied to the individual and atlas spherical maps (Van Essen, 2005).

Contrasts between tasks were based on a common metric that reflected the spatial distributions of activity in different OP regions. The metric involved nodes selected on each hemisphere's post-registration fiducial surface and especially surface area measures that manifested the unique parietal opercular anatomy in each hemisphere of every individual. We computed areas for each participant and task and separately for each OP subdivision. The activity dependent area was computed from nodes whose registered F-test z-scores equaled or exceeded a threshold used for corrected t-test z-score maps[1]. An area-proportion-index was computed that was the ratio of the area for the thresholded F-test z-scores in an individual and the area of an OP subdivision in that person. Thus, statistical analyses relied on a dependent variable that was an index defined as the ratio of suprathreshold activity dependent area to total OP subdivision area. A one-way ANOVA assessed task contributions to the distribution of proportions in each OP subdivision. Post-hoc t-tests[2], with significance levels Bonferroni corrected for multiple comparisons, contrasted the distribution of proportions between selected tasks in different OP subdivisions.

[1]We computed average z-score maps from the F-test z-scores that were registered to the PALS-B12 surface nodes. The average F-test z-scores per node were assessed with t-tests (Bosch, V. 2000. Statistical analysis of multi-subject fMRI data: assessment of focal activations. Journal of Magnetic Resonance Imaging 11: 61-64.) that were corrected for multiple tests (Bonferroni for 69,328 t-tests based on the number of nodes in the PALS-B12 cortical surface exclusive of the midline) and degrees of freedom (N-1 varied with sample size (N) per task) at a p-value threshold of 0.01. These corrected t-values were transformed into z-score maps scaled to the same p-value threshold.

[2]Error was the subject by task interaction term.

RESULTS

Parietal opercular subdivisions

Eickhoff and colleagues computed probability maps for parietal opercular cytoarchitectonic subdivisions (OP 1-4) based on cytoarchitectonic identifications in 10 postmortem brains (Eickhoff et al., 2006a; Eickhoff et al., 2006b). We registered, summed, and mapped linear transformations of these probability maps and subdivision boundaries to a standardized cortical surface-based atlas (PALS-B12 Van Essen, 2005) as described in the Appendix. Most OP regions are hidden within the depths of the Sylvian fissure. However, portions of OP 1 and 4 extend out onto the surface of lateral parietal cortex as shown on the average fiducial cortical surface in Figure 3A. Substantial inflation of the cortical surface uncovers the parietal operculum and presents a full overview of all four OP subdivisions (Figure 3B). The OP boundaries drawn in Figure 3B are enlarged and reproduced in Figure 3C together with overlays of the T-maps of F-test z-scores for each of the tasks.

All tactile tasks activated the posterior parietal operculum contralateral to the stimulated right finger pad. Many tasks also evoked activity in matching ipsilateral cortex. The distribution of this activity across the four OP subdivisions is shown in Figure 3C. Task specific differences in these T-maps are discussed below. However, consistent with the differences shown in Figure 3C, a one-way ANOVA of the area-proportion-index for each OP subdivision found significant effects by tasks in all contralateral OP subdivisions (Table 2a). The ANOVA results from OP subdivisions ipsilateral to stimulation were not significant after correction for multiple ANOVA tests. However, the area-proportion-index differences in OP 4 were close to significant at 0.05 (Table 2a). Particular task contrasts contributing to these ANOVA results on spatial extent differences are considered below.

OP 1 - The T-maps show that all tasks activated approximately the same middle portion of contralateral OP 1 (Figure 3C). However, Task 1, detecting a difference in vibration frequencies, engaged the smallest proportion of OP 1 compared especially to most other tasks. Progressively greater proportions of OP 1 were affected by Tasks 2-8, respectively. Thus, the area-proportion-index for Task 1 was ~30% of OP 1 (Figure 4), for the other vibrotactile stimulation tasks it was ~40% (Figure 4) and for all surface stimulation tasks (Tasks 5-8) it was >50% (Figure 4). For example, significantly smaller area-proportion-indices for Task 2 compared to Task 7 in post-hoc t-tests illustrate these differences between spatial extents engaged by vibrotactile and surface stimulation tasks (Table 2b). Similar spatial extent differences characterized task pairings between other vibrotactile and surface stimulation tasks (Figure 4).

The T-maps show generally less extensive task effects in ipsilateral (right) OP 1. The map was virtually blank for Task 1, sparse for the other vibrotactile stimulation tasks, largely confined to a single medial/inferior focus for surface stimulation Tasks 5-7, and most extensive for Task 8 (Figure 3C). Consistent with the T-maps, the area-proportion-index for Task 1 was ~20% of OP 1, near 30% for the remaining vibrotactile tasks, ~50% for surface stimulation tasks (Tasks 5-7), and over >60% for Task 8 (Figure 4). Despite these differences, there was no significant difference across tasks in the ANOVA for ipsilateral OP 1 (Table 2a) and, not unexpectedly, for example, between the smaller area-proportion-index for the vibrotactile Task 2 compared to the surface stimulation Task 7 in post-hoc t-tests (Table 2b) or any other comparable pairings. Although these results suggest the absence of task differences in ipsilateral OP 1, they also may indicate greater variability and possibly a smaller effect size in ipsilateral OP 1. These negative results in ipsilateral OP 1 are not explained by differences in handedness because all but one participant reported right hand dominance.

OP 2 - The T-maps show slight involvement of contralateral OP 2 for Tasks 1-7 and indicate more substantial spatial extent for Task 8 (Figure 3C). Similarly, the area-proportion-indices were all <25% for Tasks 1-7 but >50% for Task 8 (Figure 4). Consistent with these relative relationships, for example, area-proportion-index for Task 8 was significantly greater than that for Task 1 (Table 2b).

The T-maps generally revealed more of an impact on ipsilateral OP 2 (Figure 3C). A consequence was that most area-proportion-indices exceeded 25% except for Task 1. However, only the area-proportion-index during the letter identification (Task 8) was significantly greater than during the vibrotactile detection Task 1 (Table 2b). Other task contrasts (e.g., Task 2 vs. Task 8 or Task 2 vs. 7) did not differ, possibly due to greater and unequal variance amongst these task area-proportion-indices.

OP 3 - The T-maps indicated that contralateral OP 3 was affected by nearly every task, especially in its most inferior and anterior aspects (Figure 3C). The area-proportion-indices were ≤30% for all vibrotactile tasks, >40% for the two surface discrimination Tasks 6 and 7, and ~70% for the letter recognition Task 8 (Figure 4). These differences probably explain the significant ANOVA (Table 2a). In post-hoc t-tests, the area-proportion-index was significantly greater for Task 8 compared to each of the vibrotactile tasks. Comparable differences characterized other pairings between the other vibrotactile vs. surface stimulation Tasks 6 and 7.

The T-maps in ipsilateral OP 3 showed a variety of activation patterns from the different tasks. The between task variances also differed significantly, which possibly was responsible for no significant results in the ANOVA for this OP region (Table 2a). The area-proportion-index was greatest for Task 8 (Figure 4) and this was significantly greater than the <10% index for Task 1 (Table 2b).

OP 4 - The T-maps indicated that all tasks impacted OP 4 bilaterally (Figure 3C). The ANOVA (Table 2a) indicated significantly different area-proportion-indices across the tasks. In contralateral OP 4 differences possibly responsible for these ANOVA results involved area proportions of <15% for Task 1, ~30% for the remaining vibrotactile tasks and surface stimulation with a smooth surface, ~40% for the two surface discrimination Tasks 6 and 7, and ~70% for the letter recognition Task 8 (Figure 4). Post-hoc t-tests confirmed these distinctions; the area-proportion-index was significantly greater for Task 8 compared to each of the vibrotactile tasks (Table 2b). Comparable differences characterized pairings between the other vibrotactile vs. surface stimulation Tasks 6 and 7. Additionally within the vibrotactile tasks and with a more lenient, uncorrected p-value, the area-proportion-index for the least demanding frequency detection Task 1 was significantly lower than that for Task 4 (Table 2b). Similarly, in ipsilateral OP 4, area-proportion-indices ranged from ≤15% in Task 1 to ≥70% for Task 8 (Figure 4). Post-hoc t-tests indicated that within both sets of tasks significantly smaller area-proportion-indices were present in the tasks that involved possibly less discrimination complexity. Thus, the area-proportion-index for Task 1 differed significantly from that for Task 4, and similar differences were noted for Task 5 vs. Task 8 (Table 2b).

DISCUSSION

The current findings in humans confirm results from animal studies of multiple lateral parietal somatosensory subdivisions (Burton et al., 1995; Coq et al., 2004; Disbrow et al., 2003; Krubitzer et al., 1995; Qi et al., 2002; Wu and Kaas, 2003). Additionally, the distinguishable activation patterns for OP 1, 3 and 4 subdivisions strengthen the suggestion that homologues to, respectively, S2, VS and PV in monkeys exist in humans (Eickhoff et al., 2006a; Eickhoff et al., 2007). The varied extent and location of activity in these OP subdivisions also draw

attention to previously reported somatotopy in these subdivisions given tactile stimulation of the same right second finger pad in all tasks. A principal finding was that the spatial extents of activity in OP subdivisions differed by task. These response distributions potentially arose from differences in low level perceptual processes associated with vibrotactile compared to surface stimulation. Additionally, however, the cognitive demands varied across the tasks even within the sets that involved comparable stimulation protocols. Consequently, we also consider whether potential cognitive differences contributed to the observed differences in area-proportion-indices.

Somatotopy in OP Subdivisions

Consensus on somatotopy in lateral parietal cortex of monkeys is that the digits/hand map to the middle of PV and S2 with a mirror-symmetric pattern for body representations across the border between these regions (Burton et al., 1995; Coq et al., 2004; Disbrow et al., 2003; Krubitzer et al., 1995; Qi et al., 2002; Wu and Kaas, 2003). In humans, Eickhoff and colleagues noted distal body representations adjoined at the extremities at the border between OP 4 and OP 1 (Eickhoff et al., 2007). The identified representation across the border is probably coextensive with a finger-two region previously ascribed to “S2” (Disbrow et al., 2000; Ruben et al., 2001). In general, these findings were partially confirmed.

Thus, as expected the T-maps for vibrotactile and most surface stimulation tasks (e.g., Task 2-7) showed affects through the middle of contralateral OP 1. Nevertheless, these results are not entirely somatotopic. The map for Task 8 showed extensive involvement across nearly all of OP 1. Additionally, the maps in ipsilateral and contralateral OP 1 differed. The focal site in ipsilateral OP 1 was located further anterior and inferior for Tasks 3 and 5-7. Again, the T-maps for Task 8 contained no particular focus, but involved most of ipsilateral OP 1. Differences between contralateral and ipsilateral maps have not been described previously. However, the observed differences plausibly suggest that bilateral processing of tactile inputs from unilateral stimulation might involve different components of at least OP 1.

A predicted central location for the digits was only partly confirmed in OP 4. Thus, in contralateral OP 4, the principal foci were centrally located and contiguous with the group T-maps in OP 1, especially for most vibrotactile tasks and possibly the surface stimulation Tasks 6 and 7. However, there is a separate cluster as well for the vibrotactile tasks and for the surface stimulation tasks the cluster is mostly separate from the affected zone in OP 1. The foci in ipsilateral OP 4 similarly were located close, but not always adjoined to the cluster in OP 1 for several tasks (e.g., 3 and 5-8). Thus, the T-maps for most tasks only poorly instantiate a representation of adjoining digit representations at the border between OP 1 and 4. The T-maps for Task 8 diverged bilaterally from a predicted central digit zone due to widespread involvement of, especially contralateral OP 4.

Some divergence from predicted somatotopy was found for most tasks, and especially for the surface stimulation tasks. Principally, the T-maps for these tasks were more extensive than previously described hand/finger representations (Disbrow et al., 2000; Eickhoff et al., 2007). One explanation for this difference is that a greater area of the finger pad was stimulated with the moving surfaces. However, maps varied for different surface stimulation tasks despite comparable contact with the finger pad. For example, the map from stimulating with embossed letters showed no focal representation and left little of OP 1 for the rest of the body representation. Possibly greater cognitive demands associated with tactile letter recognition engaged more than a segregated representation of digit 2 in OP 1. However, even the maps noted with vibrotactile stimulation in the present study might have reflected cognitive behavior in contrast to mapping using passive tactile stimulation protocols. Thus, OP map characteristics are malleable and probably influenced by task demands even in the most topologically defined OP 1 and 4 regions.

Prior neurophysiological studies in behaving macaques also reported discrepancies in the receptive field structure of individual neurons within the component digit/hand representation in S2. Thus, intermixed within expected somatotopic areas for the digits were neurons with widespread multi-digit, hand, arm, etc receptive fields (Fitzgerald et al., 2006b; Robinson and Burton, 1980a; Sinclair and Burton, 1993). Large receptive fields for some “hand” S2 neurons were observed when monkeys actively touched and cognitively processed distributed surfaces (Sinclair and Burton, 1993). Such findings support the suggestion that cognitive tasks and/or differences in perceptual processing can influence observed somatotopy in parietal opercular subdivisions OP 1 and 4.

Maps in OP 3 occupied the superior limiting sulcus anterior to OP 1 in a site that possibly coincides with a hand representation described for either VS-rostral or caudal in monkeys (Coq et al., 2004; Qi et al., 2002; Robinson and Burton, 1980b). Somatotopy in VS-caudal is head to trunk from an anterior to posterior; a reversed posterior to anterior/head to trunk somatotopy is likely in VS-rostral (Coq et al., 2004; Qi et al., 2002; Wu and Kaas, 2003). A precise topography in OP 3 could not be determined from current data. Furthermore, OP 3 lies medial to OP 4 (PV), which contrasts with locating VS-caudal medial to S2 in monkeys (Burton et al., 1995; Coq et al., 2004; Disbrow et al., 2003; Krubitzer et al., 1995; Qi et al., 2002; Robinson and Burton, 1980a; Wu and Kaas, 2003). A hand area in OP 3 was previously based upon observing activation when stimulating the hand in one individual, but a “hand” area was not shown in a group summary “maximum likelihood representation” (Eickhoff et al., 2007). The current findings confirm activation of OP 3 from stimulating the tip of digit 2 and support identifying it as yet another lateral parietal somatosensory subdivision. However, whether OP 3 is a homologue for VS-caudal or VS-rostral is indefinite. Possibly additional somatotopic mapping will establish further correspondence to the anterior-posterior organizations previously described in monkeys for the two components of VS.

T-map results in OP 2 were especially prominent for most surface stimulation tasks, but were also obtained for several of the vibrotactile tasks. These findings suggest that OP 2 is more than a vestibular area as previously reported (Eickhoff et al., 2006c). Eickoff and colleagues discounted a somatosensory role for OP 2 because they found that tactile activation of OP 2 had the lowest mean probability compared to other parietal opercular subdivisions (Eickhoff et al., 2007). The OP 2 activity was also noted where it adjoined anticipated responses in nearby OP 3 during tactile stimulation of the legs (Eickhoff et al., 2007), which again suggested possible problems with activity registrations within the deepest/fundal parts of the parietal operculum. The OP 2 clusters noted here, especially those associated with the vibrotactile stimulation tasks, were separated from other more superficial foci, which discounts the possibility that the observed clusters were a consequence of spillover from registration misalignments of activity. An interpretation of the current findings is to suggest a possible homology for OP 2 with a caudal somatosensory area identified in animals that is located inferior and posterior to S2 (e.g., Ri or VS-caudal) (Burton et al., 1995; Coq et al., 2004; Disbrow et al., 2003; Krubitzer et al., 1995; Qi et al., 2002; Robinson and Burton, 1980a; Wu and Kaas, 2003). If this notion is correct, then OP 3 might be appropriately considered the homologue of VS-rostral.

Possible Factors Affecting Activity in OP Subdivisions

One contributing factor to the varied maps associated with the different tasks was differences in low-level stimulus features. Accordingly, tasks utilizing surface stimulation provide greater mechanical translation across the finger pad than tasks employing punctate vibrotactile stimulation and might therefore provoke more extensive activity distributions. Such low-level stimulation factors possibly contributed to the several instances of significantly smaller area-

proportion-indices for the vibrotactile compared to the surface stimulation tasks. Two findings suggest that additional factors might be involved.

First, it was not universal that the area-proportion-indices for any vibrotactile task were always smaller than those for any surface stimulation task. Thus, significant differences mostly involved contrasts between the least cognitively demanding frequency detection vibrotactile, and most surface stimulation tasks; there were no significant differences between the area-proportion-indices for the more demanding selective and divided vibrotactile attention and the surface stimulation tasks that involved discriminating grating roughness or shape differences. Secondarily, significant differences primarily involved contrasts between the cognitively more demanding letter recognition surface stimulation, vs. each vibrotactile task. Additionally, significant differences were detected between some tasks that used the same mode of stimulation and hence identical low-level perceptual features. Examples with vibrotactile stimulation involved significantly smaller area-proportion-indices for Tasks 1 vs. 4 within OP 4 bilaterally. Task 1 involved simple detection of rarely encountered trials where vibration frequencies matched. In contrast, Task 4 required more cognitive resources because both parameters of vibration frequency and duration were attended and processed in a divided tactile attention paradigm. Similarly, for tasks with surface stimulation smaller area-proportion-indices occurred for Tasks 5 or 6 vs. 8 in ipsilateral OP 4 and for Task 5 vs. 8 in contralateral OP 3. All surface stimulation tasks again involved the same low-level perceptual features; and these tasks required processing multiple surface features that had to be remembered, processed and integrated for accurate discriminations. However, recognizing embossed letters possibly entailed perceiving and remembering more shape features plus sublexical recollection.

These differences suggest that varied cognitive demands influenced the spatial extent of activity in some OP regions. A smaller area-proportion-index occurred for the task that was cognitively less demanding (e.g., Task 1). Prior human imaging studies also noted that cognitively relevant tasks elicited greater activation of “S2” (Bodegård et al., 2000; Bodegård et al., 2001; Burton et al., 2008; Ledberg et al., 1995; Nelson et al., 2004; Reed et al., 2005; Roland et al., 1998; Young et al., 2004). Fitzgerald and colleagues (Fitzgerald et al., 2004, 2006a) similarly suggested that parietal opercular neurons in macaques, which respond best to active touch, possibly contribute to higher cognition, especially when coding tactile and proprioceptive sensations derived from touching the complex features of objects. The underlying intriguing hypothesis is that activity in lateral parietal somatosensory subdivisions concerns higher cognitive processes rather than simply providing an additional somatotopic map of stimulated body parts.

ACKNOWLEDGEMENTS

We gratefully acknowledge D.G. McLaren and S. Dixit for assistance with data collection and analyses and J. Kreitler and Dr. G. Perry for the design and construction of the tactile stimulators.

Supported by NIH grants NS31005 and NS37237.

APPENDIX

Eickhoff and colleagues kindly provided subdivision parcellation for each of ten postmortem brains that were linearly registered to the Colin Montreal Neurological Institute (MNI) target. We registered the Colin MNI template to our local template (711-2B), a version of the Colin template in a standard stereotaxic space (Buckner et al., 2004) that is similar but not identical to Talairach space (Talairach and Tournoux, 1988; Van Essen and Dierker, 2007); the registration was of high quality because both source and target brains were from the same individual. The resulting affine matrix (Colin in MNI to Colin in 711-2B) was then applied to the linearly registered postmortem parcellations using FMRIB’s linear registration tool

(FLIRT, http:www.fmrib.ox.ac.uk/fsl/flirt/index.html) and nearest neighbor interpolation. These re-registered OP probability volumes were then summed to generate 711-2B probability maps that were mapped to the PALS-B12 average fiducial surface in 711-3C space, which is equivalent to 711-2B (Buckner et al., 2004). Caret's enclosing voxel mapping method was used.

Each resulting OP subdivision map was spatially smoothed by four iterations of averaging across nearest node values. Then, contiguous probability maps for each OP ROI were formed as follows: (1) sequentially subtracting from each OP subdivision the remaining three OP ROI probability maps (e.g., OP 1-OP 2, OP 1-OP 3, and OP 1-OP 4), (2) converting retained positive values from each subtraction to binary by self-division, (3) creating exclusive OP domains by multiplying the binary coded maps resulting from each set of subtractions per OP ROI, and (4) revising the probability maps by multiplying the exclusive binary OP domain with the original, un-subtracted smoothed probability map for each OP ROI.

To draw contiguous boundaries around a surface based registration of an OP ROI, all nodes associated with the subdivision were selected using a minimum probability of 10%. This criterion, imposed on the smoothed data, assured that after averaging across adjacent nodes, the retained node represented data from at least one postmortem brain. Selected nodes were assigned a unique color value, and CARET software created borders around these painted areas (Van Essen, 2005). Manual border smoothing (± 1-2 nodes) eliminated points jutting out of and into adjacent subdivisions and imposed continuous, juxtaposed boundaries between ROI. Figure 3A shows surface based registration of OP ROI painted areas and borders tucked into the parietal operculum on the PALS-B12 average fiducial surface; Figure 3B shows surface based registration of ROIs on a very inflated surface.

REFERENCES

Binkofski F, Buccino G, Posse S, Seitz R, Rizzolatti G, Freund H. A fronto-parietal circuit for object manipulation in man: evidence from an fMRI-study. European Journal of Neuroscience 1999;11:3276–3286. [PubMed: 10510191]

Bodegård A, Geyer S, Naito E, Zilles K, Roland PE. Somatosensory areas in man activated by moving stimuli: cytoarchitectonic mapping and PET. Neuroreport 2000;11:187–191. [PubMed: 10683855]

Bodegård A, Geyer S, Grefkes C, Zilles K, Roland PE. Hierarchical processing of tactile shape in the human brain. Neuron 2001;31:317–328. [PubMed: 11502261]

Bosch V. Statistical analysis of multi-subject fMRI data: assessment of focal activations. Journal of Magnetic Resonance Imaging 2000;11:61–64. [PubMed: 10676622]

Buckner RL, Head D, Parker J, Fotenos AF, Marcus D, Morris JC, Snyder AZ. A unified approach for morphometric and functional data analysis in young, old, and demented adults using automated atlas-based head size normalization: reliability and validation against manual measurement of total intracranial volume. Neuroimage 2004;23:724–738. [PubMed: 15488422]

Burton H, Videen TO, Raichle ME. Tactile-vibration-activated foci in insular and parietal-opercular cortex studied with positron emission tomography: mapping the second somatosensory area in humans. Somatosensory and Motor Research 1993;10:297–308. [PubMed: 8237217]

Burton H, Fabri M, Alloway K. Cortical areas within the lateral sulcus connected to cutaneous representations in areas 3b and 1: a revised interpretation of the second somatosensory area in macaque monkeys. Journal of Comparative Neurology 1995;355:539–562. [PubMed: 7636030]

Burton H, Sinclair RJ, McLaren DG. Cortical activity to vibrotactile stimulation: an fMRI study in blind and sighted individuals. Human Brain Mapping 2004;23:210–228. [PubMed: 15449356]

Burton H, McLaren DG, Sinclair RJ. Reading embossed capital letters: an fMRI study in blind and sighted individuals. Human Brain Mapping 2006;27:325–339. [PubMed: 16142777]

Burton H, Sinclair RJ, McLaren DG. Cortical network for vibrotactile attention: A fMRI study. Human Brain Mapping 2008;2:207–221. [PubMed: 17390318]

Coq JO, Qi H, Collins CE, Kaas JH. Anatomical and functional organization of somatosensory areas of the lateral fissure of the New World titi monkey (Callicebus moloch). Journal of Comparative Neurology 2004;476:363–387. [PubMed: 15282711]

Disbrow E, Roberts T, Krubitzer L. Somatotopic organization of cortical fields in the lateral sulcus of Homo sapiens: evidence for SII and PV. Journal of Comparative Neurology 2000;418:1–21. [PubMed: 10701752]

Disbrow E, Litinas E, Recanzone GH, Padberg J, Krubitzer L. Cortical connections of the second somatosensory area and the parietal ventral area in macaque monkeys. Journal of Comparative Neurology 2003;462:382–399. [PubMed: 12811808]

Eickhoff SB, Schleicher A, Zilles K, Amunts K. The human parietal operculum. I. Cytoarchitectonic mapping of subdivisions. Cerebral Cortex 2006a;16:254–267. [PubMed: 15888607]

Eickhoff SB, Amunts K, Mohlberg H, Zilles K. The human parietal operculum. II. Stereotaxic maps and correlation with functional imaging results. Cerebral Cortex 2006b;16:268–279. [PubMed: 15888606]

Eickhoff SB, Weiss PH, Amunts K, Fink GR, Zilles K. Identifying human parieto-insular vestibular cortex using fMRI and cytoarchitectonic mapping. Human Brain Mapping 2006c;27:611–621. [PubMed: 16281284]

Eickhoff SB, Lotze M, Wietek B, Amunts K, Enck P, Zilles K. Segregation of visceral and somatosensory afferents: an fMRI and cytoarchitectonic mapping study. Neuroimage 2006d;31:1004–1014. [PubMed: 16529950]

Eickhoff SB, Grefkes C, Zilles K, Fink GR. The somatotopic organization of cytoarchitectonic areas on the human parietal operculum. Cerebral Cortex 2007;17:1800–1811. [PubMed: 17032710]

Fitzgerald PJ, Lane JW, Thakur PH, Hsiao SS. Receptive field properties of the macaque second somatosensory cortex: evidence for multiple functional representations. Journal of Neuroscience 2004;24:11193–11204. [PubMed: 15590936]

Fitzgerald PJ, Lane JW, Thakur PH, Hsiao SS. Receptive field properties of the macaque second somatosensory cortex: representation of orientation on different finger pads. Journal of Neuroscience 2006a;26:6473–6484. [PubMed: 16775135]

Fitzgerald PJ, Lane JW, Thakur PH, Hsiao SS. Receptive field (RF) properties of the macaque second somatosensory cortex: RF size, shape, and somatotopic organization. Journal of Neuroscience 2006b; 26:6485–6495. [PubMed: 16775136]

Friston K, Holmes A, Worsley K, Poline J, Frith C, Frackowiak R. Statistical parametric maps in functional imaging: a general linear approach. Human Brain Mapping 1995;2:189–210.

Hinkley LB, Krubitzer LA, Nagarajan SS, Disbrow EA. Sensorimotor integration in S2, PV, and parietal rostroventral areas of the human sylvian fissure. Journal of Neurophysiology 2007;97:1288–1297. [PubMed: 17122318]

Holmes AP, Friston KJ. Generalisability, random effects and population inference. Neuroimage 1998;7:S754.

Inoue K, Yamashita T, Harada T, Nakamura S. Role of human SII cortices in sensorimotor integration. Clin Neurophysiol 2002;113:1573–1578. [PubMed: 12350433]

Krubitzer L, Clarey J, Tweedale R, Elston G, Calford M. A redefinition of somatosensory areas in the lateral sulcus of macaque monkeys. Journal of Neuroscience 1995;15:3821–3839. [PubMed: 7751949]

Krubitzer LA, Sesma MA, Kaas JH. Microelectrode maps, myeloarchitecture, and cortical connections of three somatotopically organized representations of the body surface in parietal cortex of squirrels. Journal of Comparative Neurology 1986;250:403–430. [PubMed: 3760247]

Krubitzer LA, Calford MB. Five topographically organized fields in the somatosensory cortex of the flying fox: microelectrode maps, myeloarchitecture, and cortical modules. Journal of Comparative Neurology 1992;317:1–30. [PubMed: 1573055]

Kwong KK, Belliveau JW, Chesler DA, Goldberg IE, Weisskoff RM, Poncelet BP, Kennedy DN, Hoppel BE, Cohen MS, Turner R, Cheng H-M, Brady TJ, Rosen BR. Dynamic magnetic resonance imaging of human brain activity during primary sensory stimulation. Proceedings of the National Academy of Sciences USA 1992;89:5675–5679.

Ledberg A, O'Sullivan BT, Kinomura S, Roland PE. Somatosensory activations of the parietal operculum of man. A PET study. European Journal of Neuroscience 1995;7:1934–1941. [PubMed: 8528469]

Miezin FM, Maccotta L, Ollinger JM, Petersen SE, Buckner RL. Characterizing the hemodynamic response: effects of presentation rate, sampling procedure, and the possibility of ordering brain activity based on relative timing. Neuroimage 2000;11:735–759. [PubMed: 10860799]

Nelson AJ, Staines WR, Graham SJ, McIlroy WE. Activation in SI and SII: the influence of vibrotactile amplitude during passive and task-relevant stimulation. Cognitive Brain Research 2004;19:174–184. [PubMed: 15019713]

Ogawa S, Lee TM, Kay AR, Tank DW. Brain magnetic resonance imaging with contrast dependent on blood level oxygenation. Proceedings of the National Academy of Sciences USA 1990;87:9868–9872.

Ojemann JG, Akbudak E, Snyder AZ, McKinstry RC, Raichle ME, Conturo TE. Anatomic localization and quantitative analysis of gradient refocused echo-planar fMRI susceptibility artifacts. Neuroimage 1997;6:156–167. [PubMed: 9344820]

Ollinger JM, Shulman GL, Corbetta M. Separating processes within a trial in event-related functional MRI. II. Analysis. Neuroimage 2001a;13:210–217. [PubMed: 11133323]

Ollinger JM, Corbetta M, Shulman GL. Separating processes within a trial in event-related functional MRI. I. The method. Neuroimage 2001b;13:218–229. [PubMed: 11133324]

Qi HX, Lyon DC, Kaas JH. Cortical and thalamic connections of the parietal ventral somatosensory area in marmoset monkeys (Callithrix jacchus). Journal of Comparative Neurology 2002;443:168–182. [PubMed: 11793354]

Raczkowski D, Kalat JW, Nebes R. Reliability and validity of some handedness questionnaire items. Neuropsychologia 1974;12:43–47. [PubMed: 4821188]

Reed CL, Klatzky RL, Halgren E. What vs. where in touch: an fMRI study. Neuroimage 2005;25:718–726. [PubMed: 15808973]

Robinson CJ, Burton H. Somatotopographic organization in the second somatosensory area of M. fascicularis. Journal of Comparative Neurology 1980a;192:43–67. [PubMed: 7410613]

Robinson CJ, Burton H. Organization of somatosensory receptive fields in cortical areas 7b, retroinsula, postauditory and granular insula of M. fascicularis. Journal of Comparative Neurology 1980b; 192:69–92. [PubMed: 7410614]

Roland PE, O'Sullivan B, Kawashima R. Shape and roughness activate different somatosensory areas in the human brain. Proceedings of the National Academy of Sciences USA 1998;95:3295–3300.

Ruben J, Schwiemann J, Deuchert M, Meyer R, Krause T, Curio G, Villringer K, Kurth R, Villringer A. Somatotopic organization of human secondary somatosensory cortex. Cerebral Cortex 2001;11:463–473. [PubMed: 11313298]

Sinclair RJ, Burton H. Neuronal activity in the second somatosensory cortex of monkeys (Macaca mulatta) during active touch of gratings. Journal of Neurophysiology 1993;70:331–350. [PubMed: 8360718]

Talairach, J.; Tournoux, P. Coplanar Stereotaxic Atlas of the Human Brain. Thieme Medical; New York: 1988.

Van Essen DC, Dickson J, Harwell J, Hanlon D, Anderson CH, Drury HA. An integrated software system for surface-based analyses of cerebral cortex. Journal of American Medical Informatics Association 2001;8:443–459.

Van Essen DC. A population-average, landmark- and surface-based (PALS) atlas of human cerebral cortex. Neuroimage 2005;28:635–662. [PubMed: 16172003]

Van Essen DC, Dierker DL. Surface-based and probabilistic atlases of primate cerebral cortex. Neuron 2007;56:209–225. [PubMed: 17964241]

Vega-Bermudez F, Johnson KO, Hsiao SS. Human tactile pattern recognition: active versus passive touch, velocity effects, and patterns of confusion. Journal of Neurophysiology 1991;65:531–546. [PubMed: 2051193]

Wasaka T, Nakata H, Akatsuka K, Kida T, Inui K, Kakigi R. Differential modulation in human primary and secondary somatosensory cortices during the preparatory period of self-initiated finger movement. European Journal of Neuroscience 2005;22:1239–1247. [PubMed: 16176367]

Wu CW, Kaas JH. Somatosensory cortex of prosimian Galagos: physiological recording, cytoarchitecture, and corticocortical connections of anterior parietal cortex and cortex of the lateral sulcus. Journal of Comparative Neurology 2003;457:263–292. [PubMed: 12541310]

Young JP, Herath P, Eickhoff S, Choi J, Grefkes C, Zilles K, Roland PE. Somatotopy and attentional modulation of the human parietal and opercular regions. Journal of Neuroscience 2004;24:5391–5399. [PubMed: 15190112]

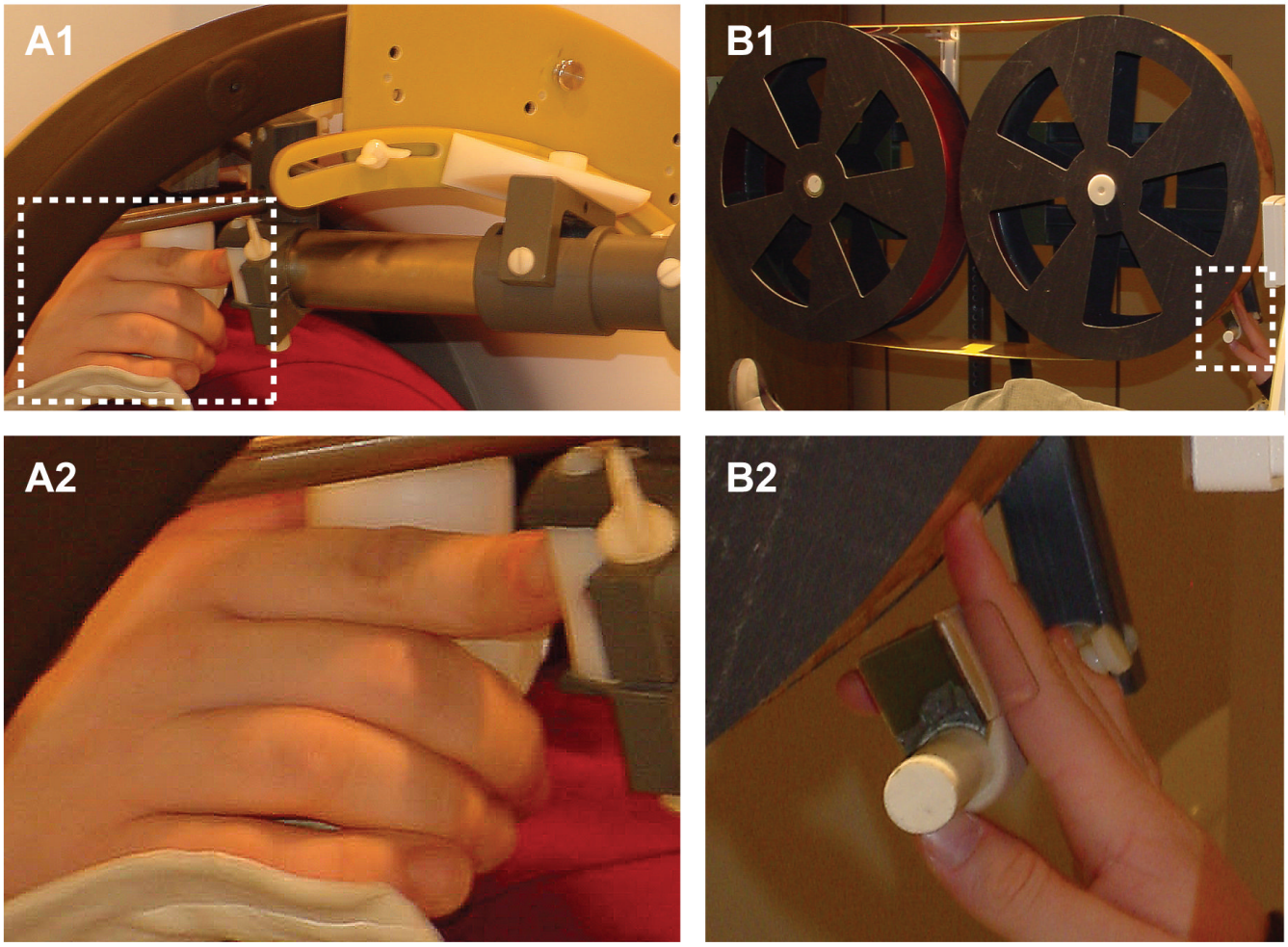

Figure 1.

Mechanical stimulators. **A1.** The vibrator used for vibrotactile stimulation consisted of a titanium shaft that floated on an air-bearing. The latter were housed inside the shown outer titanium tube. A magnetically and electrically shielded electromechanical driver (not shown) was attached to the shaft and was displaced 12 feet from the scanner. **A2.** The finger rested against a platform with a central annulus for the probe tip. The platform was attached to the outer tube. **B1.** The rotating drum used for surface stimulation consisted of a continuous flexible photopolymer belt that snugly fitted over two fiberglass cylinders. A shielded stepper motor driver (not shown) was attached to the axel of the cylinder located furthest from the scanner. **B2.** The finger rested in a small channel whose position could be adjusted to align the finger tip with a selected track along the belt circumference.

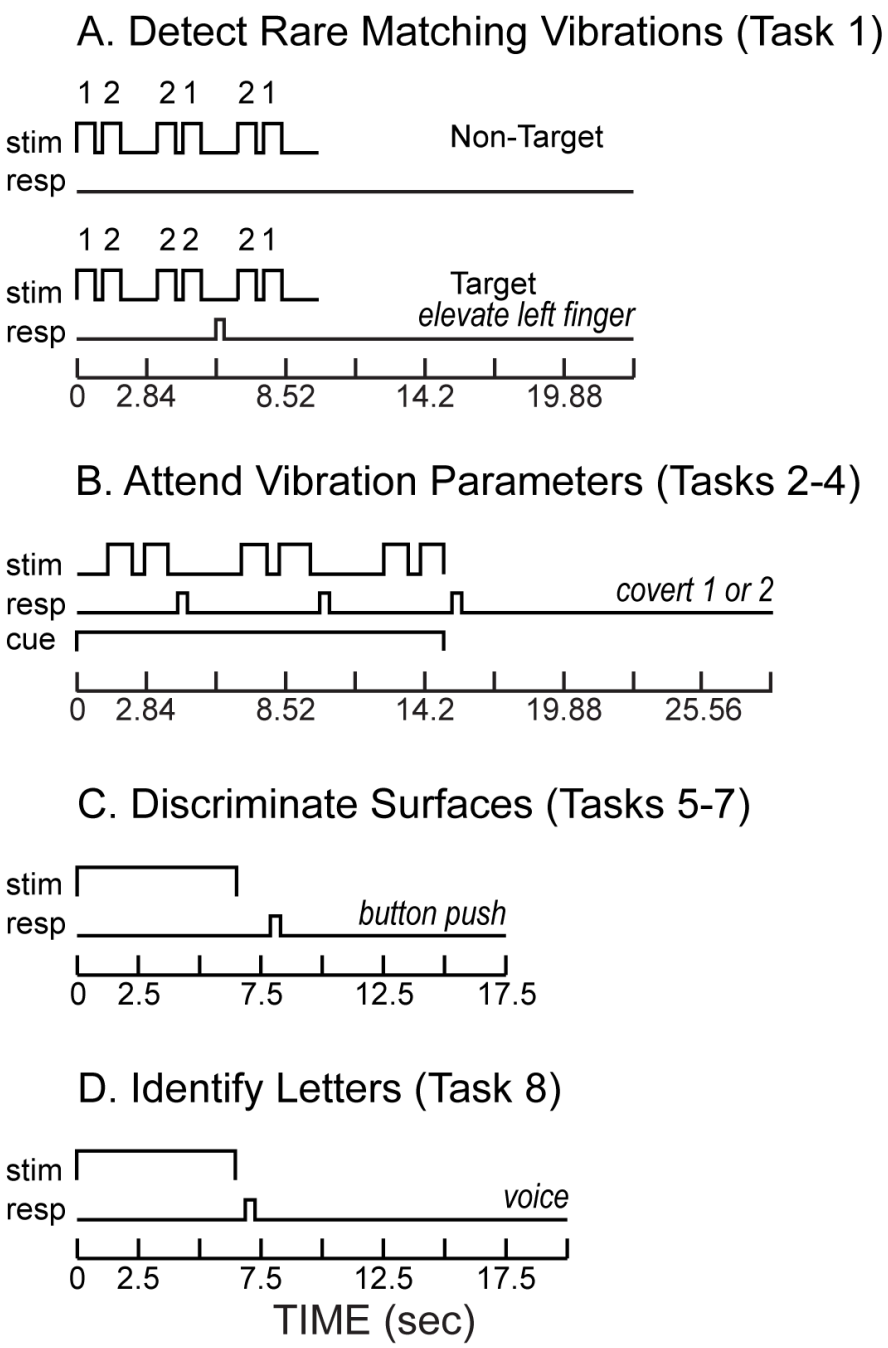

Figure 2.

Timelines for tactile stimulation tasks. **A.** Task 1 involved three trials of paired vibration stimulation (stim) in each event. Two vibration frequencies were used (1= 25Hz and 2= 100Hz). Detection of matched paired vibration frequencies required elevation of a left hand finger (resp). Events containing any trial with matched frequencies were coded as a Target; events where all three trials contained unmatched frequencies were coded as a Non-Target. **B.** Tasks 2-4 involved three trials of paired vibrotactile stimulation that were similarly cued (cue).Vibration parameters of frequency and duration varied for each pair. Cuing instructed whether attention was to be directed to one or both vibration parameters in order to detect the temporal order of the stimulation at a higher frequency or longer duration vibration. Covert

responses of “1” or “2” indicated whether the target parameter was first or second in a pair. **C.** Surface stimulation events involved epochs of rotary translation of a 40mm segment of a photopolymer surface across the finger pad. Each imaging run was dedicated to a different surface pattern (Task 5: smooth, Task 6: horizontal gratings, Task 7: shapes). Identification of specified surface patterns required button pushes (resp) with the left second or third fingers. **D.** Surface stimulation involved rubbing with a string of 6 identical embossed capital letters. Voiced identification of the letter name in Task 8 was recorded and deconstructed with noise suppression software (Burton et al., 2006).

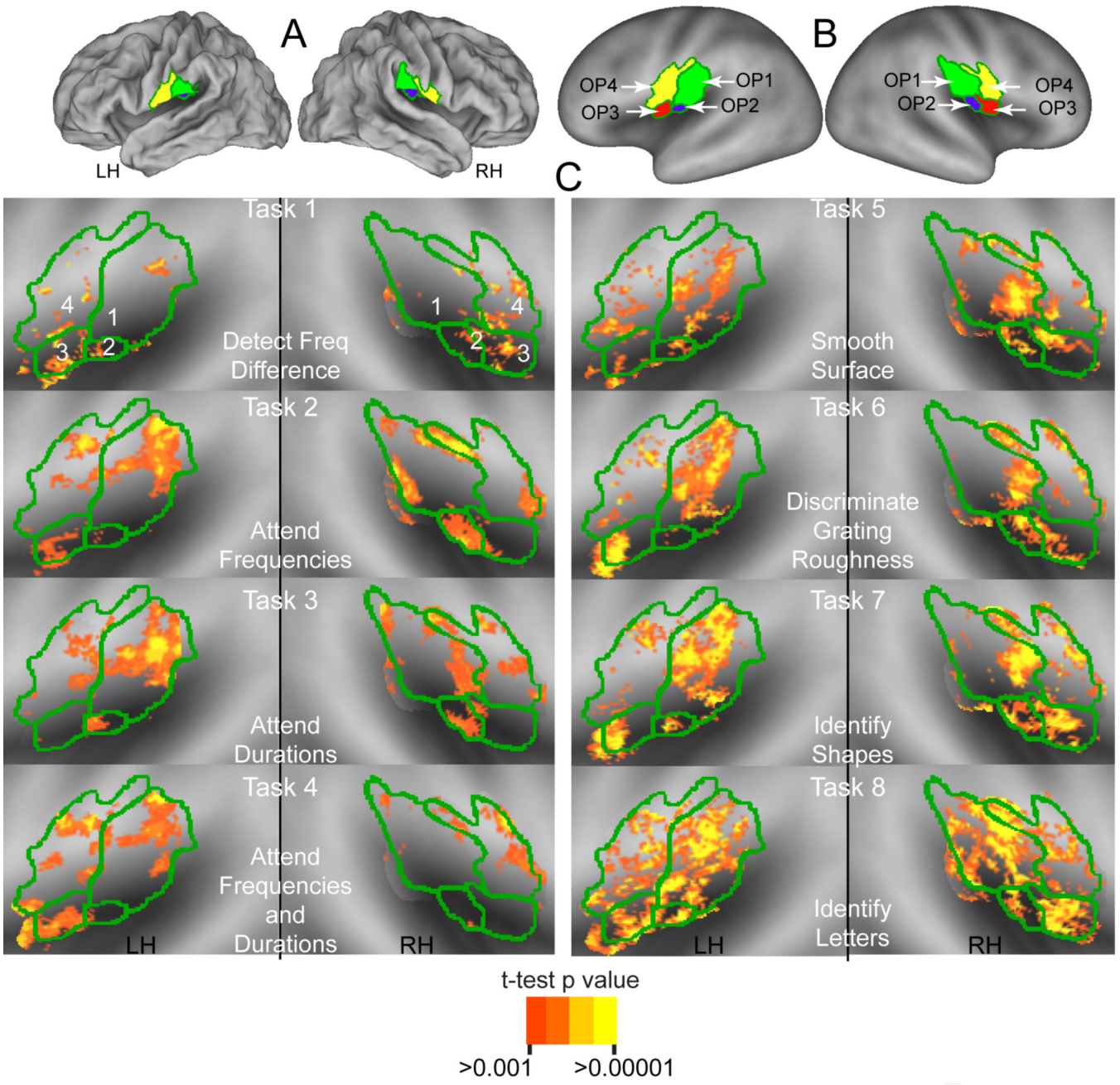

Figure 3.

OP ROI mapped to PALS-B12 atlas together with group average random effect t-test maps during different tasks. **A.** OP 1 and 4 are partly visible in a lateral view of PALS-B12 average fiducial cortical surface (Van Essen, 2005). **B.** A full overview of all 4 OP regions is visible on a very inflated PALS-B12 average cortical surface. Green borders and different colors mark the boundaries of OP subdivisions. **C.** T-maps in OP 1-OP 4 for different tasks. Numbers 1-4 in C, respectively label OP 1-4.

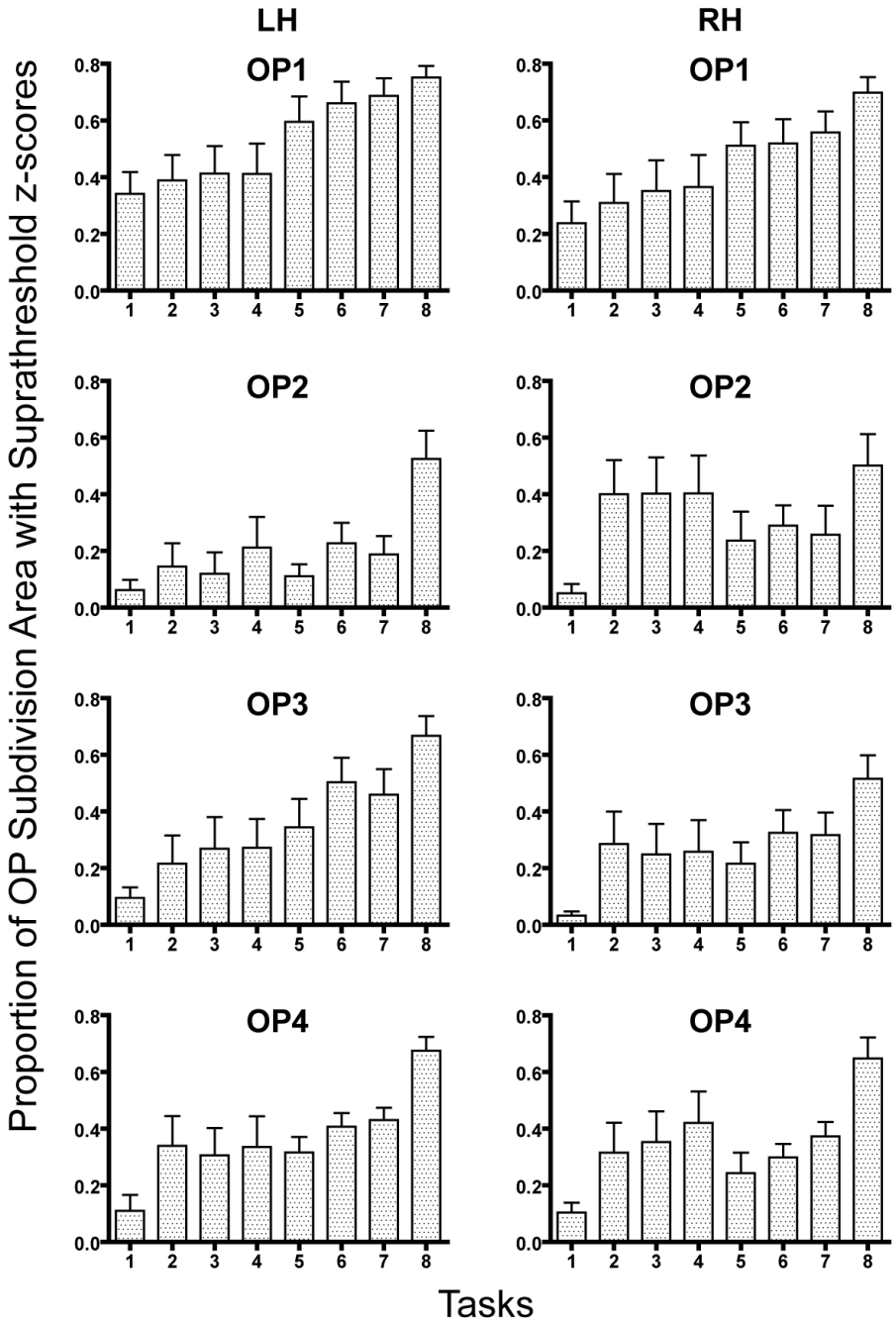

Figure 4.
Area-proportion-indices by OP subdivision and task. Bars show means and SEM.

Table 1

Data sets and image acquisition parameters

TASKS	**1**	**2-4**	**5-7**	**8**
	detect freq difference	attend freq/duration	smooth, gratings, shapes	letters
Sample size (N)	8 (8 male)	12 (8 male)	10 (6 male)	10 (7 male)
Age, Yr	45.5 ±4.5	28.3 ±3.7	18.5 ±1.2	43.2 ±5.2
Right Handed (mean, SE)	85.1, 8.8	92.8, 4.9	94.6, 1.3	70.4, 10.5
Mean Accuracy	>75%	>75%*	>95%	>85%
Scanner	3T, Allegra	1.5, Vision	3T, Allegra	3T, Allegra
EPI:				
TR/TE ms	2840/30	~2800/50	2048/25	2500/30
Flip Angle	90°	90°	90°	90°
Slices/Voxel size, mm	32/ 4 × 4 × 4	21/ 3.75 × 3.75 × 6	32/ 4 × 4 × 4	32/ 4 × 4 × 4
Time points per run	167	328	193	154
No. runs per event-type	4	4	2	2
Trials per event-type	68	32	48	38

* Performance accuracy in prior training sessions.

Table 2

Table 2a. One-way ANOVA				
Side	**Subdivision**	**F**	**df**	**p**
LH	OP 1	3.35	7, 76	0.0144
	OP 2	2.97	7, 76	0.0332
	OP 3	3.4	7, 76	0.0132
	OP 4	3.35	7, 76	0.0144
RH	OP 1	2.5	7, 76	0.0916
	OP 2	1.32	7, 76	1.0000
	OP 3	1.38	7, 76	0.9100
	OP 4	2.73	7, 76	0.0556

Table 2b. Student t-tests					
Side	**Subdivision**	**Task Contrast**	**t**	**df**	**p**
LH	OP 1	2 vs. 7	2.63	20	0.0081
	OP 2	1 vs. 8	4.38	16	0.0010
	OP 3	3 vs. 8	6.69	16	<0.0001
	OP 4	1 vs. 4	1.59	18	0.048
	OP 4	4 vs. 8	2.86	20	0.0080
	OP 4	5 vs. 8	1.6	18	0.0640
RH	OP 1	2 vs. 7	0.37	22	0.3587
	OP 2	1 vs. 8	3.79	16	0.0015
	OP 3	3 vs. 8	1.91	20	0.0354
	OP 4	1 vs. 4	2.14	18	0.0230
	OP 4	4 vs. 8	1.64	20	0.0588
	OP 4	5 vs. 8	3.93	18	0.0005

*Shaded cells significant after multiple comparison correction.